NJC
New Journal of Chemistry

A journal for new directions in chemistry

Accepted Manuscript

This article can be cited before page numbers have been issued, to do this please use: L. Invernizzi, C. Damiano, G. Manca and E. Gallo, *New J. Chem.*, 2025, DOI: 10.1039/D5NJ03189C.

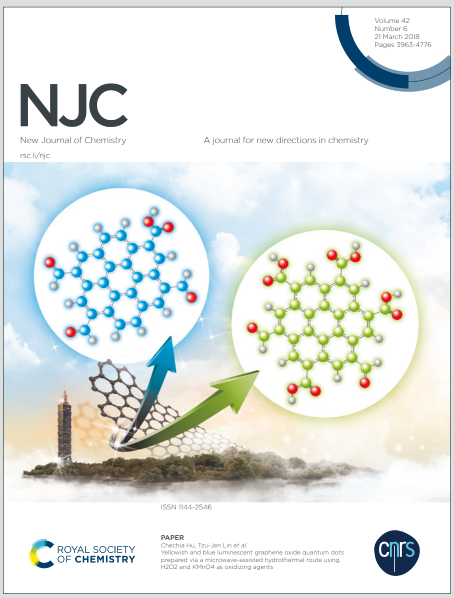

View Article Online
DOI: 10.1039/D5NJ03189C

ARTICLE

Activating Harmful Small Molecules Under Mild Conditions: Theoretical Insights into Cinchonine-based Valorization of CO_2, CS_2, and COS

aReceived 00th January 20xx,
Accepted 00th January 20xx

DOI: 10.1039/x0xx00000x

Lucia Invernizzi,[a] Caterina Damiano,*[a] Gabriele Manca*[b] and Emma Gallo[a]

DFT calculations have been employed to deeply investigate the mechanism of CO_2 cycloaddition to aziridines catalyzed by cinchonine hydrochloride salt, forming oxazolidin-2-ones under ambient conditions (room temperature, 0.1 MPa CO_2). Computed energy barriers align with experimental observations and support a dual activation mechanism involving hydrogen bonding and nucleophilic attack at the aziridine carbon atom. The theoretical study also accounts for the observed regioselectivity, rationalizing the preference for nucleophilic attack at the more substituted aziridine carbon atom. Consistent with experimental findings, the calculations reveal that the reaction efficiency is influenced by the nature of the substituent at the aziridine nitrogen atom, explaining the lack of reactivity observed with *N*-aryl aziridines due to steric and electronic factors that hamper the reaction. Furthermore, the DFT study suggests that COS and CS_2 can be activated for analogous cycloaddition reactions. Although these transformations involve higher energy barriers compared to that of the CO_2 cycloaddition, the formation of oxazolidin-2-thiones and thiazolidin-2-thiones is predicted to be feasible under slightly elevated temperatures (for CS_2) or near-ambient conditions (for COS). These findings highlight the potential of cinchonine hydrochloride salt as an efficient, biocompatible and cost-effective catalyst for the sustainable valorization of small harmful molecules under mild conditions.

Introduction

The activation of small molecules has long been a central theme in chemical research, driven by the challenge of breaking strong bonds in simple, thermodynamically stable species. Historically, much of this work has focused on inert molecules such as N_2, O_2 and CH_4, which are starting materials in processes like nitrogen fixation, oxidation reactions, and hydrocarbon functionalization.[1,2] During the last decades, scientific interest has progressively moved toward carbon dioxide. Although CO_2 is similarly unreactive, it presents a distinctive combination of scientific and environmental urgency. Its massive atmospheric abundance, mainly due to anthropogenic emissions, and its well-established role in global warming have made its activation a priority in the context of sustainable chemistry. As a result, CO_2 is now viewed not only as a waste product but also as a potential carbon feedstock, whose efficient transformation could contribute to both climate mitigation and resource circularity.

Advances in catalytic[3-5] and electrochemical methods[6-8] have enabled the efficient conversion of CO_2 into a variety of useful chemicals[9] and fuels[10] such as carbon monoxide, formic acid, methanol, methane, and a range of value-added compounds. In light of the development of a circular and sustainable economy, the establishment of new and efficient processes for the CO_2 valorization has become interesting for the synthesis of fine chemicals. One particularly intriguing reaction is the 100% atom-efficient cycloaddition of CO_2 into organic substrates, such as epoxides[11-12] and aziridines,[13-20] to produce high-value chemicals like cyclic carbonates and oxazolidin-2-ones, respectively, which have several applications including as pharmaceutical agents.[21-23] Classic CO_2 activation typically requires the co-presence of an electrophilic and a nucleophilic promoter. In the synthesis of oxazolidin-2-ones, the electrophile, generally a metal center, interacts with nitrogen aziridine atom to render one of the two carbon atoms more susceptible to nucleophilic attack. The consequent cleavage of the C–N bond transfers electron density to the nitrogen atom, which in turn becomes capable of activating the CO_2 molecule (Scheme 1). The need for both electrophilic and nucleophilic functionalities led to the development of various binary and bifunctional metal-based catalysts for the CO_2 cycloaddition to aziridines.[4-10,13] More recently metal-free systems,[14-15,18-19,24] which integrate both functional components enabling efficient aziridine activation and ring-opening without the use of external metal catalysts, have also been extensively developed. Although CO_2 has received widespread attention as a platform molecule for sustainable synthesis, its thio-analogous, carbon disulfide (CS_2) and carbonyl sulfide (COS), have remained largely overlooked.

[a] Department of Chemistry, University of Milan, Via C. Golgi 19, 20133 Milan (Italy) E-mail: caterina.damiano@unimi.it
[b] Istituto di Chimica dei Composti Organo Metallici – CNR-ICCOM Sede Secondaria di Bari, c/o Dipartimento di Chimica, Università degli Studi di Bari, Via Orabona 4, 70126 Bari (Italy) E-mail: gmanca@iccom.cnr.it

Supplementary Information available: [details of any supplementary information available should be included here]. See DOI: 10.1039/x0xx00000x

View Article Online
DOI: 10.1039/D5NJ03189C

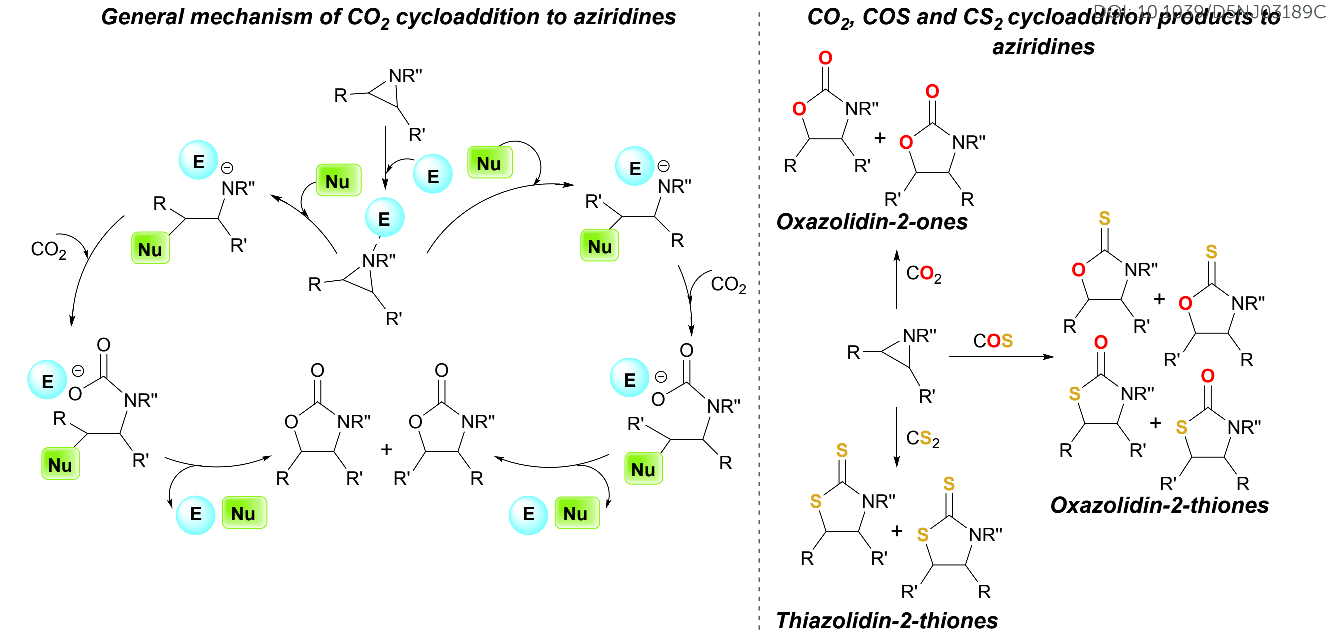

Scheme 1: General reaction mechanism of CO_2 cycloaddition to aziridines (left); CO_2, COS and CS_2 cycloaddition products to aziridines (right).

Since the early 1970s, when the reactivity of CS_2 toward aziridines was first investigated,[25,26] research on COS and CS_2 has primarily focused on their interactions with metal complexes.[27,28] Only in recent years the interest in these triatomic molecules has expanded, with growing attention to their cycloaddition reactions with epoxides and aziridines, particularly *via* metal-organic framework (MOF)-based catalytic systems in combination with nucleophilic co-catalysts.[29-32] The limited experimental examples reported for the CS_2 cycloaddition to aziridines rely on expensive binary systems involving amidato divalent lanthanide complexes, among which the most active is represented by the europium derivative used in combination with DBU (1,8-diazabiciclo[5.4.0]undec-7-ene).[29] Other examples include cerium-based framework,[30] porous 3D cobalt-organic framework assembled by $[Co_{15}]$ and $[Co_{18}]$ nanocages[31] and 3D material assembled by twisted cylindrical $[Dy_{24}]$ cages.[32] In all cases, TBAB (tetrabutylammonium bromide) was the co-catalyst; either the metal centre or the positive channel of the MOF-based material act as a Lewis acid to activate the aziridine, while the external nucleophile promotes the ring-opening reaction enabling the CS_2 insertion and the product formation. To date, no examples of active bifunctional organocatalytic systems have been reported. The above-described behavior aligns with the structural and electronic similarities between COS, CS_2, and CO_2, highlighting their potential for analogous activation and transformation pathways.[27,29,33] It is important to note that CS_2 and COS not only cause environmental effects but can also contribute to various health disorders, particularly affecting the human reproductive and nervous systems.[34,35] Therefore, rather than eliminating them through traditional combustion methods, treating and reusing these compounds as carbon and sulfur resources offers an attractive alternative to reduce the presence of toxic sulfur-containing pollutants in the atmosphere. In this view, CS_2 and COS could serve as valuable C1-building blocks for the synthesis of sulfur-containing heterocycles,[36-38] such as thiazolidin-2-thiones and oxazolidin-2-thiones (Scheme 1), and other functionalized materials,[39] offering new opportunities in the field of small-molecule activation and sustainable sulfur chemistry.

It is important to underline that the activation of small molecules such as CO_2, CS_2, and COS, should occur under mild reaction conditions to ensure a favorable balance between the energy required for the transformation and the amount of CO_2 effectively utilized. If harsh conditions are employed, such as high temperatures, elevated pressures, or energy-intensive inputs, the environmental benefit of using these molecules as feedstocks may be offset by additional CO_2 emissions generated during the process. For this reason, the development of catalytic systems capable of operating efficiently under ambient or near-ambient conditions is essential to maximize the net carbon benefit and make these transformations truly viable from both an energetic and environmental standpoint.

Given the growing demand for low-toxicity synthetic procedures, the use of eco-friendly bifunctional organocatalysts has become increasingly attractive. Recently, we reported a combined experimental and computational investigation of the catalytic properties of the metal-free *bis*-protonated porphyrin $TPPH_4Cl_2$ (TPP = dianion of tetraphenylporphyrin) in promoting the cycloaddition of CO_2 into *N*-alkyl aziridines to produce *N*-alkyl oxazolidin-2-ones at 100 °C and 1.2 MPa of CO_2 pressure.[16] Computational analysis revealed that the reaction occurred thanks to a porphyrin/aziridine synergic CO_2 activation in which the protonated core of porphyrin acts, by establishing hydrogen bonding with the CO_2 oxygen atom, as electrophilic center to facilitate the nucleophilic attack of the aziridine

View Article Online
DOI: 10.1039/D5NJ02689C

nitrogen atom to the CO_2 carbon atom. The study paved the way to develop other bifunctional organocatalytic systems, bearing the same nucleophilic moiety (chloride anion) but different electrophilic NH^+-containing species, to promote the synthesis of *N*-alkyl oxazolidin-2-ones at milder experimental conditions.[40] In this context, some of us recently published a study on the catalytic activity of hydrochloride salts of DBU, quinine, and cinchonine,[40] which were active at room temperature and 0.1 MPa of CO_2 pressure. In view of the very good results achieved, we decided to investigate the electronic/energetic features of the mechanism of these reactions by using DFT calculations. In addition, the potential catalytic activity of cinchonine hydrochloride salt to promote the cycloaddition of other triatomic harmful molecules such as CS_2 and COS has been investigated *in silico*. The obtained computational results pave the way for developing future efficient and eco-compatible catalytic processes for the synthesis of fine chemicals by recycling waste.

Results and Discussion

Cycloaddition of CO_2 to 1-butyl-2-phenylaziridine (1_{butyl}) promoted by cinchonine hydrochloride (3)

In light of remarkable data published for the synthesis *N*-alkyl oxazolidin-2-ones under mild experimental conditions,[40] a detailed computational analysis was carried out on the model CO_2 cycloaddition to 1-butyl-2-phenylaziridine (**1_{butyl}**) yielding 3-butyl-5-phenyloxazolidin-2-ones (**$2A_{butyl}$** + **$2B_{butyl}$**) (Scheme 2), catalyzed by the naturally derived cinchonine hydrochloride salt (**3**). Although particular emphasis was placed on elucidating the reaction mechanism catalyzed by **3**, the mechanisms involving hydrochloride salts of DBU and quinine, organocatalysts **4** and **5** respectively, were also investigated and collected data are reported in the Supporting Information. The structures of **3**, **4**, and **5** organocatalysts were optimized at the B97D-DFT level of theory[41] and shown in Figure 1. The solvent effects have been taken into account by using CPCM model[42-43] for acetonitrile, that is the solvent employed in experimental studies already published on the CO_2 cycloaddition to aziridines.[40] Additional methodological details are provided in the Supporting Information.

According to the published experimental results,[40] 1-butyl-2-phenylaziridine (**1_{butyl}**) was chosen as the model substrate to investigate the catalytic mechanism of the reaction promoted by **3**, and CH_3CN was the modeled reaction solvent.

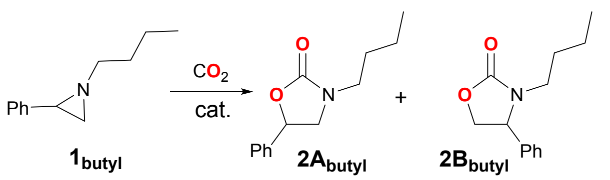

Scheme 2: Synthesis of 3-butyl-5-phenyloxazolidin-2-ones **$2A_{butyl}$** and **$2B_{butyl}$** by CO_2 cycloaddition to 1-butyl-2-phenylaziridine (**1_{butyl}**).

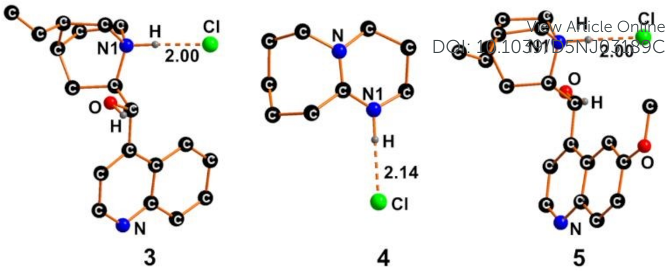

Figure 1: Optimized structure of hydrochloride salts **3**, **4** and **5**. The hydrogen atoms were hidden for the sake of clarity, except for those linked to heteroatoms. Selected distances are given in Å.

Drawing from prior data on the $TPPH_4Cl_2$-mediated reaction,[16] the first step of the computational analysis focused on the possible formation of adduct **6_{butyl}** in which CO_2 is positioned between hydrochloride salt **3** and aziridine **1_{butyl}**. As shown in Figure 2, **6_{butyl}** was computationally identified with a free energy cost of +15.0 kcal mol^{-1} resulting from a balance between the favorable enthalpic contribution of -6.5 kcal mol^{-1} and a severe unfavorable entropic contribution. The local electrophilicity index (ω_K^+) of the two aziridine carbon atoms, namely C2 and C3, was estimated by using the method developed by Domingo *et al.*[44]

The calculations revealed that the ω_K^+ value for C2 is twofold higher than that of C3, suggesting a more favored nucleophilic attack at C2 rather than at C3 carbon atom. This is in line with the experimentally observed reaction regioselectivity,[40] as 3-butyl-5-phenyloxazolidin-2-one (compound **$2A_{butyl}$** in Scheme 2) was always detected as the major isomer. Consequently, the mechanism yielding isomer **$2B_{butyl}$**, deriving from the nucleophilic attack on C3, was not further studied by DFT calculations.

In adduct **6_{butyl}**, aziridine nitrogen atom N2 acts as a nucleophile toward CO_2, which loses its linearity with the O-C1-O angle reduced to 135°, as confirmed by the appearance of an IR-active vibration at 1759 cm^{-1}, associated with the asymmetric stretching of the C–O bonds. The chloride anion remains distant from the C2 center, with a Cl···C2 distance of 3.76 Å whose reduction to 2.80 Å revealed the presence of a transition state, designated **$TS_{6-7butyl}$** (Figure 3).

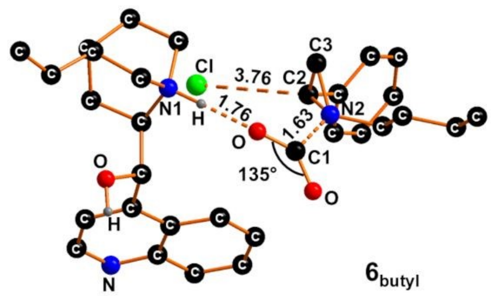

Figure 2: Optimized structure of adduct **6_{butyl}**. The hydrogen atoms were hidden for the sake of clarity, except for those linked to a heteroatom. Selected distances are given in Å and O-C1-O angle in degrees (°).

View Article Online
DOI: 10.1039/D5NJ03189C

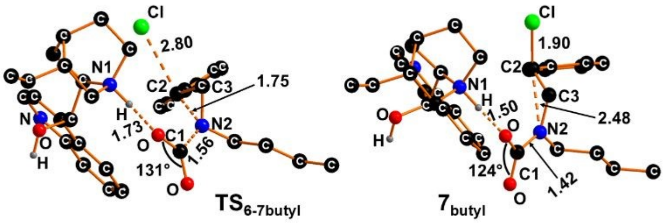

Figure 3: Optimized structure of transition state **TS**$_{6-7butyl}$ and intermediate **7**$_{butyl}$. The hydrogen atoms were hidden for the sake of clarity, except for those linked to a heteroatom. Selected distances are given in Å and O-C1-O angle in degrees (°).

In **TS**$_{6-7butyl}$, the approaching chloride anion weakens the N2–C2 bond, which is elongated by 0.15 Å compared to adduct **6**$_{butyl}$. This facilitates the initial shift of electron density toward the aziridine nitrogen N2, enhancing its nucleophilicity toward CO_2. This effect is further supported by a 0.07 Å shortening of the N2···C1 distance and a more pronounced bending of the CO_2 moiety, with the O-C-O angle reduced by 4° with respect to adduct **6**$_{butyl}$. From an energetic perspective, the transition from **6**$_{butyl}$ to **TS**$_{6-7butyl}$ involves an estimated free energy barrier of +4.3 kcal mol^{-1}. The transition state nature of **TS**$_{6-7butyl}$ was confirmed by the presence of a single imaginary frequency at -170 cm^{-1}, corresponding to the approach of the chloride ion to C2 atom and the complete cleavage of the C2–N2 bond. Following **TS**$_{6-7butyl}$, the system evolves toward the minimum-energy structure **7**$_{butyl}$ (Figure 3) that displays the complete formation of the C2–Cl bond (1.90 Å) and the corresponding cleavage of the N2···C2 bond (2.48 Å). The C1–N2 bond is also fully formed, with a length of 1.42 Å. The formation of intermediate **7**$_{butyl}$ was estimated to be exergonic, with a free energy change of -12.6 kcal mol^{-1}. At this point, the electron density originally localized on the N2 center has shifted toward the oxygen atoms of the original CO_2 moiety, leading to a strengthening of the O···H hydrogen bond, as indicated by a 0.23 Å shortening compared to the corresponding distance in **TS**$_{6-7butyl}$.

As confirmed by this O···H shortening, the oxygen atom of intermediate **7**$_{butyl}$ becomes electron-rich and capable of performing a nucleophilic attack to the C2 center yielding oxazolidin-2-one **2A**$_{butyl}$ by a ring-closure step and the regeneration of catalyst **3**. Intermediate **8**$_{butyl}$ (Figure 4) was achieved through the formation of the transition state **TS**$_{7-8butyl}$, whose structure was computationally identified (Figure 4).

In **TS**$_{7-8butyl}$, the O-C2-Cl moiety adopts a *quasi*-linear arrangement with an angle of 165°, and the C2 atom approaches a *quasi*-planar geometry. The nucleophilic approach of oxygen atom to C2 initiates the displacement of the chloride ion with an associated free energy barrier of +7.4 kcal mol^{-1}. The transition state nature of **TS**$_{7-8butyl}$ is supported by the presence of a single imaginary frequency at -216 cm^{-1}, corresponding to the formation of the O–C2 bond and the cleavage of the C2–Cl bond. Subsequently, intermediate **8**$_{butyl}$ is obtained with a free energy gain of -20.1 kcal mol^{-1} (Figure 4).

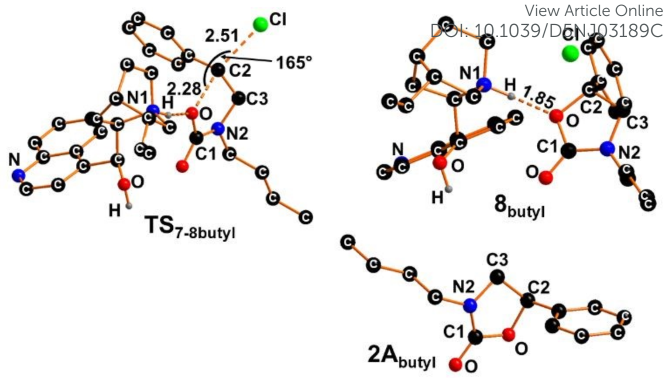

Figure 4: Optimized structure of transition state **TS**$_{7-8butyl}$, intermediate **8**$_{butyl}$ and product **2A**$_{butyl}$. The hydrogen atoms were hidden for the sake of clarity, except for those linked to a heteroatom. Selected distances are given in Å and O-C1-O angle in degrees (°).

The complete release of 3-butyl-5-phenyloxazolidin-2-one (**2A**$_{butyl}$) from **8**$_{butyl}$ is exergonic by -5.1 kcal mol^{-1} accompanied by the restoration of the salt **3**, able to perform the activation of a new aziridine moiety. The overall free energy gain, associated with the complete catalytic cycloaddition of CO_2 to 1-butyl-2-phenyl aziridine **1**$_{butyl}$ yielding **2A**$_{butyl}$, was estimated to be exergonic by -11.2 kcal mol^{-1} (Figure 5).

The energy profile of the reaction (Figure 5) reveals that the largest cost for the synthesis of **2A**$_{butyl}$ is +19.3 kcal mol^{-1}, with the main disfavoring contribution associated with the formation of the initial adduct **6**$_{butyl}$. For comparison purposes, the cycloaddition of CO_2 to **1**$_{butyl}$ was also investigated in the presence of catalysts **4** and **5**. The free energy pathways for the three catalytic processes are reported in the Supporting Information (Figure S1). No substantial changes in free energy were identified, except for the free energy stabilization of compounds analogous of intermediate **7**$_{butyl}$, namely **7'**$_{butyl}$ (involving catalyst **4**) and **7"**$_{butyl}$ (involving catalyst **5**) within 6 kcal mol^{-1}. The maximum free energy costs are within +20.8 kcal mol^{-1}, corresponding to the formation of compounds **6'**$_{butyl}$ and **6"**$_{butyl}$, analogous of the initial adduct **6**$_{butyl}$, and the subsequent transition states **TS**$_{6'-7'butyl}$ and **TS**$_{6"-7"butyl}$. The energy barriers for **TS**$_{6'-7'butyl}$ and **TS**$_{6"-7"butyl}$ fall within the range of +6.2 to +9.2 kcal mol^{-1}. All the free energy values associated with the single step of the processes are listed in Figure S2.

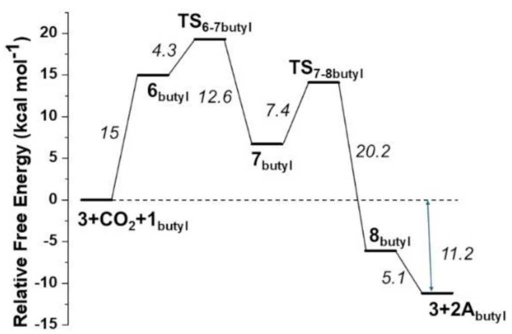

Figure 5: Free energy (kcal mol^{-1}) pathway for the cycloaddition reaction of CO_2 to 1-butyl-2-phenyl aziridine **1**$_{butyl}$ yielding 3-butyl-5-phenyloxazolidin-2-one **2A**$_{butyl}$.

View Article Online
DOI: 10.1039/D5NJ03189C

Effect of the N-aziridine substituent on the reaction efficiency

Already published experimental data[40] highlighted that the steric and electronic nature of the substituent on the aziridine nitrogen center may drastically influence the reaction efficiency. No conversion was observed when 1-(3,5-*bis*(trifluoromethyl)phenyl)-2-phenyl aziridine (**1**$_{aryl}$) was used in the CO_2 cycloaddition catalyzed by **3**. In contrast, when a cyclohexyl substituent was present at the nitrogen atom, the reaction proceeded with a low efficiency, affording the corresponding oxazolidin-2-one in 21% yield.[40] To clarify the influence of the substituent at the aziridine nitrogen atom on the reaction efficiency, a DFT computational analysis was carried out. The study was run as already described for the reaction involving 1-butyl-2-phenylaziridine **1**$_{butyl}$. First, two adducts with structures like that of **6**$_{butyl}$ were optimized by reacting CO_2 and **3** either with 1-(3,5-*bis*(trifluoromethyl)phenyl)-2-phenylaziridine (**1**$_{aryl}$) or 1-cyclohexyl-2-phenylaziridine (**1**$_{cyhexyl}$), obtaining **6**$_{aryl}$ and **6**$_{cyhexyl}$ respectively. As shown in Figure 6, the optimized structure of **6**$_{aryl}$ displays an N2---C1 distance as large as 3.02 Å, as well as a very weak hydrogen bond between H(NH$^+$) and O(CO_2), with an H---O distance of 2.64 Å.

These features, together with the nearly unperturbed linear structure of the CO_2 moiety, suggest that the occurrence of the process is unlikely when an aryl substituent is present at the N2 aziridine center, in line with the experimental results. For this reason, the CO_2 cycloaddition to 1-(3,5-*bis*(trifluoromethyl)phenyl)-2-phenylaziridine was not investigated further. Conversely, when 1-cyclohexyl-2-phenylaziridine is the involved substrate, the adduct **6**$_{cyhexyl}$ exhibits an activated CO_2 characterized by a bent O-C-O structure with an angle of 135° and a computed IR-active stretching at 1746 cm^{-1}. From the energy viewpoint, the formation of adduct **6**$_{cyhexyl}$ requires a free energy cost of +19.2 kcal mol^{-1}, higher than that needed for achieving adduct **6**$_{butyl}$ from 1-butyl-2-phenylaziridine (+15 kcal mol^{-1}). Even in this case, the obtained results are in line with experimental data, which highlighted a less efficient process when 1-cyclohexyl-2-phenylaziridine was employed as the starting material instead of 1-butyl-2-phenylaziridine.

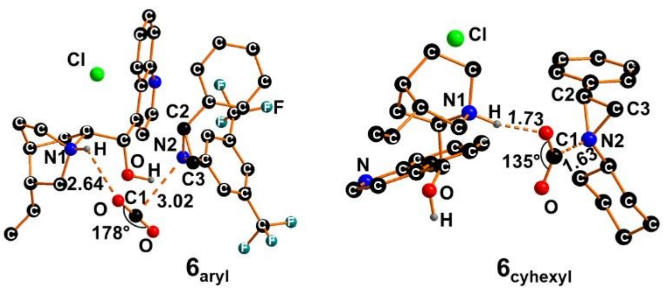

Figure 6: Optimized structure of adducts **6**$_{aryl}$ and **6**$_{cyhexyl}$, presenting 1-(3,5-*bis*(trifluoromethyl)phenyl)-2-phenylaziridine and 1-cyclohexyl-2-phenylaziridine, respectively. The hydrogen atoms were hidden for the sake of clarity, except for those linked to a heteroatom. Selected distances are given in Å and O-C1-O angle in degrees (°).

The free energy barrier for evolving from **6**$_{cyhexyl}$ to the transition state **TS**$_{6\text{-}7cyhexyl}$, whose optimized structure is reported in Figure S3, is estimated to be +6.5 kcal mol^{-1} while the overall energy barrier for transforming the starting reagents into **TS**$_{6\text{-}7cyhexyl}$ is +25.7 kcal mol^{-1}, a quite high value for a reaction performed at room temperature. The whole free energy associated with the formation of oxazolidin-2-one **2A**$_{cyhexyl}$ from 1-cyclohexyl-2-phenylaziridine (**1**$_{cyhexyl}$) and CO_2 is less exergonic than that of the same process involving 1-butyl-2-phenyl aziridine **1**$_{butyl}$ (-7.5 kcal mol^{-1} *versus* -11.2 kcal mol^{-1}). The complete energy profile of the CO_2 cycloaddition to 1-cyclohexyl-2-phenyl aziridine is reported in Figure S4.

Cycloaddition of CS_2 to 1-butyl-2-phenylaziridine (1$_{butyl}$) promoted by cinchonine hydrochloride (3)

A precedent computational analysis has predicted the feasibility, at least *in silico*, of the CS_2 cycloaddition to *N*-alkyl aziridines to provide thiazolidin-2-thiones in the presence of bifunctional **TPPH$_4$Cl$_2$**.[45] The study revealed a free energy contribution of -22.1 kcal mol^{-1} associated with the cycloaddition of CS_2 to 1-butyl-2-phenylaziridine **1**$_{butyl}$ to provide the corresponding thiazolidin-2-thione **9A**$_{butyl}$.[45] Based on these results, we studied the reaction between CS_2 and 1-butyl-2-phenylaziridine **1**$_{butyl}$ also in the presence of catalyst **3**. In this regard, the adduct **10**$_{butyl}$ (Figure 7) was optimized. Despite the favorable enthalpic contribution of -2.1 kcal mol^{-1}, adduct **10**$_{butyl}$ was optimized with a free energy cost of +21.5 kcal mol^{-1}. It should be noted that the energy cost is 6.5 kcal mol^{-1} larger than that of the analogous process involving CO_2 (formation of adduct **6**$_{butyl}$), possibly due to a weaker hydrogen bonding between the proton of **3** and the sulfur atom of CS_2, as confirmed by the long S---H distance of 2.28 Å.

After the formation of adduct **10**$_{butyl}$, the activated aziridine substrate can be attacked by chloride nucleophile through a transition state **TS**$_{10\text{-}11butyl}$ (Figure 8) with a free energy barrier of +7.7 kcal mol^{-1}. The overall barrier of +29.2 kcal mol^{-1} for the conversion of the reactants into **TS**$_{10\text{-}11butyl}$ was larger than that calculated for CO_2 activation and it can be overcome by performing the reaction at higher experimental temperatures. Transition state **TS**$_{10\text{-}11butyl}$ features a *quasi*-linear Cl-C2-N2 arrangement with an angle of 151° and a weakening of the C2-N2 bond, whose length is stretched by 0.15 Å compared to that in **10**$_{butyl}$. In **TS**$_{10\text{-}11butyl}$ the chloride approaches the C2 atom with a consistent shortening of Cl---C2 distance by 1.0 Å.

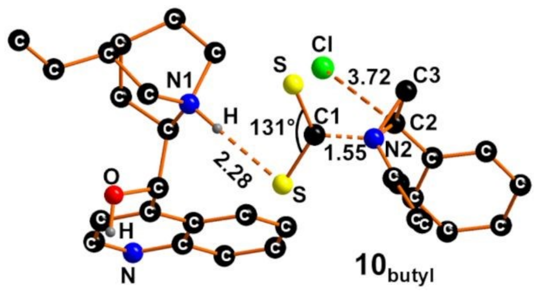

Figure 7: Optimized structure of adduct **10**$_{butyl}$. The hydrogen atoms were hidden for the sake of clarity, except for those linked to a heteroatom. Selected distances are given in Å and O-C1-O angle in degrees (°).

View Article Online
DOI: 10.1039/D5NJ03189C

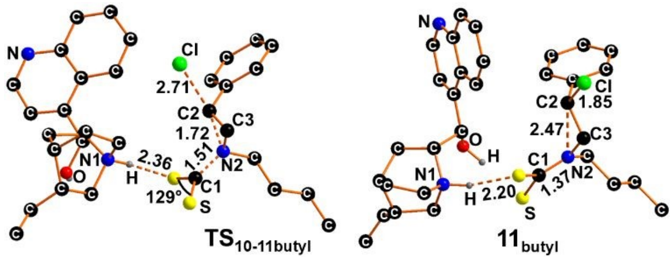

Figure 8: Optimized structure of transition state **TS$_{10\text{-}11butyl}$** and of intermediate **11$_{butyl}$**. The hydrogen atoms were hidden for the sake of clarity, except for those linked to a heteroatom. Selected distances are given in Å and O-C1-O angle in degrees (°).

The complete formation of the C2-Cl bond in intermediate **11$_{butyl}$** (Figure 8) was estimated to be exergonic by -25.9 kcal mol^{-1}.

Similarly to the CO_2 activation, the sulfur atom in **11$_{butyl}$** may perform a nucleophilic attack on the C2 center to form the 5-membered ring and regenerate the catalyst **3**. The transition state **TS$_{11\text{-}12butyl}$**, shown in Figure S5, was obtained with a free energy barrier of +13.6 kcal mol^{-1}, while the intermediate **12$_{butyl}$** (Figure 9) was obtained with the large free energy gain of -29.9 kcal mol^{-1}.

The complete release of thiazolidin-2-thione **9A$_{butyl}$**, shown in Figure 9, was achieved with a further free energy gain of -9.1 kcal mol^{-1}. The overall formation of compound **9A$_{butyl}$** by CS_2 cycloaddition to aziridine **1$_{butyl}$** is depicted in Figure 10.

A comparison between the energy profiles of CS_2 (Figure 10) and CO_2 (Figure 5) cycloaddition to **1$_{butyl}$** reveals key differences. While a higher barrier is required for the formation of the initial adduct **10$_{butyl}$** and to reach the transition state **TS$_{10\text{-}11butyl}$** in case of CS_2 activation, after more energy is released during CS_2 activation rather than during CO_2 activation. In summary, *in silico* analysis predicts that the energy barriers for the catalytic cycloaddition of CS_2 to aziridine rings are not prohibitively high, although temperatures above room temperature might be necessary to promote the reaction.

Cycloaddition of COS to 1-butyl-2-phenylaziridine (1$_{butyl}$) promoted by cinchonine hydrochloride (3)

Until now, only the activation of symmetric triatomic molecules has been investigated. This raises the question if the reaction can also proceed when a non-symmetric substrate, such as carbonyl sulfide COS, is used in the cycloaddition to aziridines.

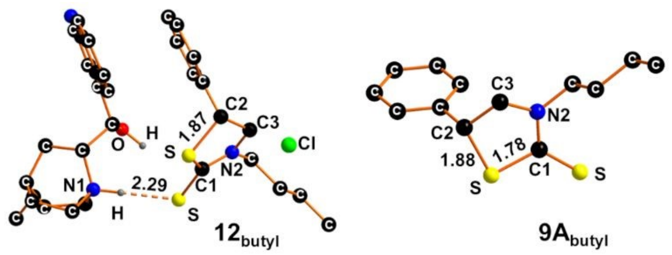

Figure 9: Optimized structure of the intermediate **12$_{butyl}$** and thiazolidin-2-thione, **9A$_{butyl}$**. The hydrogens were hidden for the sake of clarity, except for those linked to a heteroatom. Selected distances are given in Å and O-C1-O angle in degrees (°).

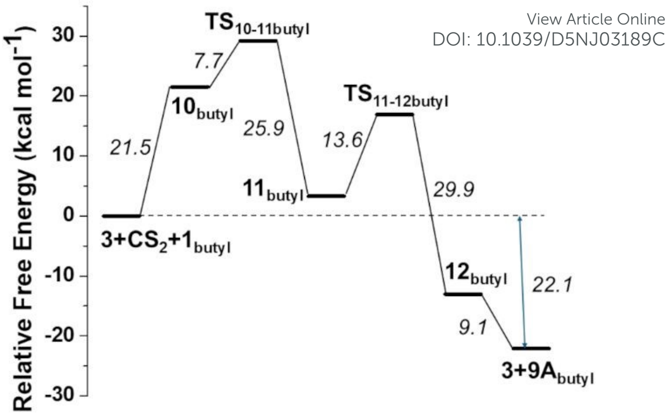

Figure 10: Free energy (kcal mol^{-1}) pathway for the cycloaddition reaction of CS_2 to 1-butyl-2-phenyl aziridine **1$_{butyl}$** forming thiazolidin-2-thione **9A$_{butyl}$**.

Unlike previous cases, different structural isomers can be obtained starting from 1-butyl-2-phenylaziridine **1$_{butyl}$** and COS. Depending on which heteroatom is involved in the cyclization step, 3-butyl-5-phenylthiazolidin-2-one (**13A$_{butyl}$**) or 3-butyl-5-phenyloxazolidin-2-thione (**14A$_{butyl}$**) can be formed (Figure 11).

To begin the computational analysis of the reaction between COS and **1$_{butyl}$**, both compounds shown in Figure 11 were optimized. Isomers **13B$_{butyl}$** and **14B$_{butyl}$**, deriving from the nucleophilic attack to the less electrophilic carbon atom C3 of the aziridine ring, were not theoretically modelled in view of the unfavorable energy costs related to their formation (see below). Preliminary DFT calculations revealed that product **13A$_{butyl}$** is more stable than **14A$_{butyl}$** by 10.4 kcal mol^{-1} in free energy. Although the energy difference between the two potential products is significant, the processes yielding both isomers were investigated. Given the non-symmetrical nature of COS, both adducts **15$_{butyl}$** (evolving in **13A$_{butyl}$**) and **16$_{butyl}$** (evolving in **14A$_{butyl}$**) (Figure 12) were optimized, featuring the alternative involvement of either oxygen or sulfur in hydrogen bonding, respectively. Adduct **15$_{butyl}$** was estimated to be 1.3 kcal mol^{-1} more stable than **16$_{butyl}$**, mainly due to a more efficient hydrogen bonding when oxygen, rather than sulfur, is involved. Starting from the reactants, adduct **15$_{butyl}$** is obtained with a free energy cost of +15.9 kcal·mol^{-1}, while the formation of **16$_{butyl}$** requires a slightly higher cost of +17.2 kcal·mol^{-1}. For adduct **15$_{butyl}$**, the N2–C2 bond cleavage *via* nucleophilic attack of chloride proceeds through transition state **TS$_{15\text{-}17butyl}$** (Figure S6) with an associated free energy barrier of +5.8 kcal·mol^{-1}. The system then evolves toward intermediate **17$_{butyl}$** (Figure 13), with a free energy gain of -16.7 kcal·mol^{-1}. Accordingly, an overall energy barrier of +21.7 kcal·mol^{-1} must be overcome to reach **TS$_{15\text{-}17butyl}$** from the separate reactants.

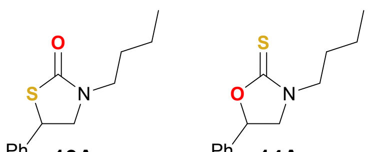

13A$_{butyl}$ **14A$_{butyl}$**

Figure 11: Potential products of the cycloaddition of COS to 1-butyl-2-phenylaziridine (**1$_{butyl}$**).

View Article Online
DOI: 10.1039/D5NJ03189C

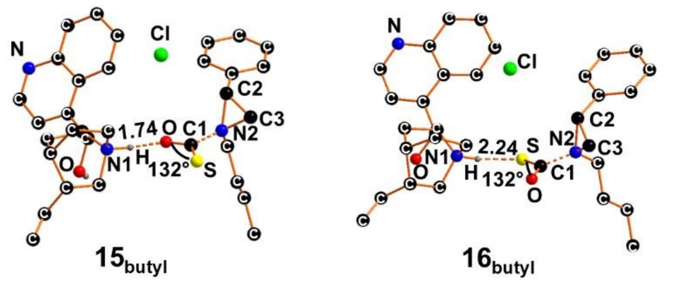

Figure 12: Free energy (kcal mol^{-1}) pathway for the cycloaddition reaction of CS_2 to 1-butyl-2-phenyl aziridine $\mathbf{1_{butyl}}$ forming thiazolidin-2-thione $\mathbf{9A_{butyl}}$. Selected distances are given in Å and O-C1-O angle in degrees (°).

Accordingly, an overall energy barrier of +21.7 kcal mol^{-1} must be overcome to reach $\mathbf{TS_{15\text{-}17butyl}}$ from the separate reactants. The potential nucleophilic attack of chloride on C3 center has been also investigated highlighting a free energy barrier of +17.8 kcal mol^{-1} to obtain $\mathbf{TS_{15\text{-}17butylC3}}$, shown in Figure S6, from adduct $\mathbf{15_{butyl}}$. Being the overall estimated free energy barrier for reaching $\mathbf{TS_{15\text{-}17butylC3}}$ is as high as +33.7 kcal mol^{-1}, this mechanism was discarded.

In the case of adduct $\mathbf{16_{butyl}}$, where the sulfur atom is involved in hydrogen bonding, the estimated free energy barrier for reaching $\mathbf{TS_{16\text{-}18butyl}}$ is +11.5 kcal mol^{-1}, resulting in an overall barrier of +28.7 kcal mol^{-1} from the isolated reactants to $\mathbf{TS_{16\text{-}18butyl}}$. The system then proceeds to intermediate $\mathbf{18_{butyl}}$, with a free energy gain of -25.4 kcal mol^{-1}. Thus, in view of the quite high calculated barrier compared to that of $\mathbf{TS_{15\text{-}17butyl}}$, the energy pathway for the formation of $\mathbf{14A_{butyl}}$ was discarded.

Starting from $\mathbf{17_{butyl}}$, the transition state $\mathbf{TS_{17\text{-}19butyl}}$ was computed with a free energy barrier of +7.9 kcal mol^{-1}, in which the sulfur center of COS can perform a nucleophilic attack to the C2 center yielding the intermediate $\mathbf{19_{butyl}}$ that evolves into the final product 3-butyl-5-phenylthiazolidin-2-one $\mathbf{13A_{butyl}}$. The complete release of $\mathbf{13A_{butyl}}$ and restoration of catalyst **3** is accompanied by a free energy gain of -6.9 kcal mol^{-1}. A complete free energy pathway for the production of 3-butyl-5-phenylthiazolidin-2-one $\mathbf{13A_{butyl}}$, starting from COS and aziridine $\mathbf{1_{butyl}}$ promoted by metal-free **3** is depicted in Figure 14 and shows an overall free energy gain of -20.8 kcal mol^{-1}.

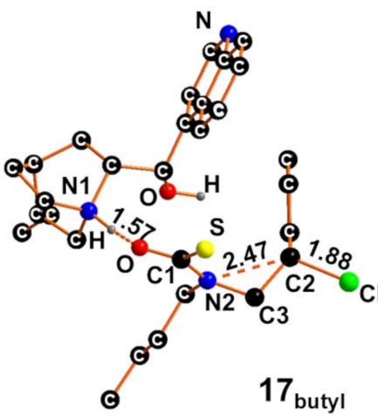

Figure 13: Optimized structure of the intermediate $\mathbf{17_{butyl}}$. The hydrogens were hidden for the sake of clarity, except for those linked to a heteroatom center Selected distances are given in Å and O-C1-O angle in degrees (°).

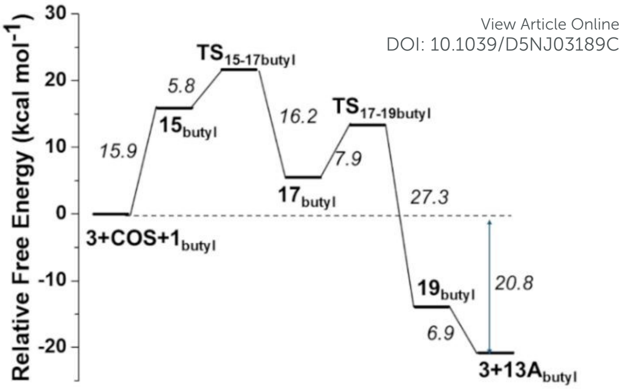

Figure 14: Free energy (kcal mol^{-1}) pathway for the cycloaddition reaction of COS to 1-butyl-2-phenyl aziridine $\mathbf{1_{butyl}}$ forming $\mathbf{13A_{butyl}}$.

To better summarize and compare the reactivity of the investigated triatomic molecules, the energy profiles of their cycloaddition to 1-butyl-2-phenyl aziridine $\mathbf{1_{butyl}}$ catalyzed by **3**, were superimposed in Figure 15.

A clear difference in overall energy gains can be observed between the formation of oxazolidine-2-one $\mathbf{2A_{butyl}}$ and its sulfur-containing analogous ($\mathbf{9A_{butyl}}$ and $\mathbf{13A_{butyl}}$). Overall energies gain calculated for CS_2 and COS cycloaddition to $\mathbf{1_{butyl}}$ resulted nearly twice higher than that of CO_2 (-20.8 kcal mol^{-1} and -22.1 kcal mol^{-1} *versus* -11.2 kcal mol^{-1}) suggesting a thermodynamic preference for the formation of oxazolidin-2-thiones and thiazolidin-2-thiones over oxazolidin-2-ones.

However, the activation barrier computed for the formation of the key transition state was higher for CS_2 (+29.2 kcal mol^{-1}) compared to CO_2 (+19.3 kcal mol^{-1}), indicating that more forcing reaction conditions may be required to achieve the product formation. In contrast, the energy barrier to reach the first transition state from COS is only slight larger than that calculated for CO_2 (+21.7 kcal mol^{-1} *versus* +19.3 kcal mol^{-1}) suggesting that its cycloaddition could proceed efficiently under the similar mild conditions successfully employed for the **3**-catalyzed oxazolidin-2-one synthesis. These findings support the feasibility of COS cycloaddition to aziridines promoted by catalyst **3** under experimental conditions only slightly more drastic than those validated for CO_2 transformations.

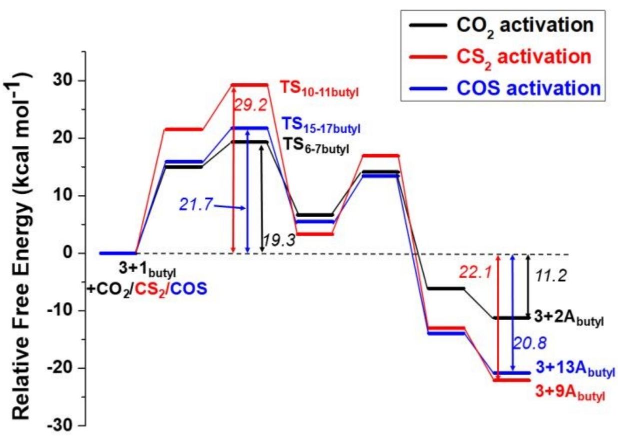

Figure 15: Superimposed free energy (kcal mol^{-1}) profiles of the cycloaddition reaction of CO_2, COS and CS_2 to 1-butyl-2-phenyl aziridine $\mathbf{1_{butyl}}$ catalyzed by **3**.

View Article Online
DOI: 10.1039/D5NJ03189C

Conclusions

In conclusion, the energetic/structural DFT analyses suggest a mechanism for the CO_2 cycloaddition to aziridine ring for the synthesis of oxazolidin-2-ones that is efficiently promoted by cinchonine hydrochloride **3** under very mild conditions (RT and 0.1 MPa of CO_2 pressure). The calculated energy barriers are compatible to the employed experimental conditions and the DFT study confirmed the double activation of CO_2 through hydrogen bonding interactions and nucleophile attack of aziridine nitrogen atom to the CO_2 carbon atom. The theoretical analysis explains the dependence of the catalytic efficiency on the steric hindrance and/or electronic effects of the *N*-aziridine substituents giving a rationale of the lack of reactivity of *N*-aryl aziridines that was experimentally observed.

To extend the activation of triatomic molecules mediated by **3** from CO_2 to CS_2 and COS, the DFT study reported here will be fundamental for managing in a near future experimental reactions involving CS_2 and COS, which until now have only been theoretically predicted. The computational analysis revealed that catalyst **3** could represent a potential candidate for efficiently mediating both CS_2 and COS activation. Even if theoretical calculations underlined that both processes involve higher energy barriers than those optimized for the CO_2 activation, acquired data support a future experimental study on the CS_2 and COS cycloaddition to aziridine in the presence of **3**. By comparing the calculated energy barriers, the cycloaddition of COS is predicted to be feasible at temperatures close to the ambient one, under conditions therefore similar to those observed for the **3**-catalyzed valorization of CO_2. In contrast, the use of CS_2 would require slightly higher temperatures. In both cases, the synthesis of thiazolidin-2-thiones and oxazolidin-2-thiones is predicted to be feasible using an inexpensive and biocompatible catalyst, such as cinchonine hydrochloride salt (**3**), under mild reaction conditions.

Conflicts of interest

There are no conflicts to declare.

Data availability

The data supporting this article have been included as part of the Supporting Information.

Acknowledgements

CD and EG thank Università degli Studi di Milano for the PSR 2023 grants.

References

1 X. B. Li, Z. K. Xin, S. G. Xia, X. Y. Gao, C. H. Tung, L. Z. Wu, *Chem. Soc. Rev.*, 2020, **49**, 9028-9056.
2 L. Wang, W. Chen, D. Zhang, Y. Du, R. Amal, S. Qiao, J. Wu, Z. Yin, *Chem. Soc. Rev.*, 2019, **48**, 5310-5349.
3 D. Intrieri, C. Damiano, P. Sonzini, E. Gallo, *J Porphyr Phthalocyanines*, 2019, **23**, 305-328.
4 C. Damiano, M. Cavalleri, L. Invernizzi, E. Gallo, *Eur. J. Org. Chem.* 2024, **27**, e202400616.
5 T. Yan, H. Liu, Z. X. Zeng, W. G. Pan, *J. CO2 Util.*, 2023, **68**, 102355.
6 K. Wiranarongkorn, K. Eamsiri, Y. S. Chen, A. Arpornwichanop, *J. CO2 Util.,* **71,** 2023, 102477.
7 L. Li, X. Li, Y. Sun, Y. Xie, *Chem. Soc. Rev.*, 2022, **51**, 1234–1252
8 L. Rotundo, R. Gobetto, C. Nervi, *Curr. Opin. Green Sustain. Chem.*, 2021, **31**, 100509.
9 Q. Zhang, X. Jin, *Chem. Eur. J.*, 2025, **31**, e202500933
10 M. Aresta, A. Dibenedetto, E. Quaranta, *J. Catal.,* 2016, **343**, 2–45.
11 S. Kaewsai, V. D' Elia, *J. Organomet. Chem.,* 2025, **1039**, 123799.
12 W. Natongchai, D. Crespy, V. D' Elia, *Chem. Commun*., 2025, **61**, 419.
13 S. Arayachukiat, P. Yingcharoen, S. V.C. Vummaleti, L. Cavallo, A. Poater, V. D'Elia, *Molecular Catalysis*, 2017, **443**, 280–285.
14 P. Yingcharoen, W. Natongchai, A. Poater, V. D' Elia *Catal. Sci. Technol*., 2020, **10**, 5544-5558.
15 C. Damiano, P. Sonzini, G. Manca, E. Gallo, *Eur. J. Org. Chem,* 2021, **2021**, 2807–2814.
16 M. Cavalleri, C. Damiano, G. Manca, E. Gallo, *Chem. Eur. J.,* 2023, **29**, e202202729
17 C. Damiano, P. Sonzini, M. Cavalleri, G. Manca, E. Gallo, *Inorg. Chim. Acta,* 2022, **540**, 121065.
18 P. Sonzini, C. Damiano, D. Intrieri, G. Manca, E. Gallo, *Adv. Synth. Catal.,* 2020, **362**, 2961–2969.
19 P. Sonzini, N. Berthet, C. Damiano, V. Dufaud, E. Gallo, *J Catal.*, 2022, **414**, 143–154.
20 C. Damiano, A. Fata, M. Cavalleri, G. Manca, E. Gallo, *Catal. Sci. Technol.,* 2024, **14**, 3996–4006.
21 A. Z. Bialvaei, M. Rahbar, M. Yousefi, M. Asgharzadeh, H. S. Kafil, *J. Antimicrob. Chemother.,* 2017, **72**, 354–364.
22 D. McBride, T. Krekel, K. Hsueh, M. J. Durkin, *Expert Opin. Drug Metab. Toxicol.,* 2017, **4**, 491.
23 F. Moureau, J. Wouters, D. Vercauteren, S. Collin, G. Evrard, F. Durant, F. Ducrey, J. Koenig, F. Jarreau, *Eur. J Med. Chem.* 1992, **27**, 939–948.
24 G. Bresciani, M. Bortoluzzi, G. Pampaloni, F. Marchetti, *Org. Biomol. Chem.* 2021, **19**, 4152–4161.
25 C. S. Dewey, R. A. Bafford, *J. Org. Chem.* 1965, **30**, 491–495.
26 T. A. Foglia, L. M. Gregory, G. Maerker, S. F. Osman, *J. Org. Chem.* 1971, **36**, 1068–1072.
27 K. K. Pandey, *Coord. Chem. Rev.* 1995, **140**, 37–114.
28 M. Guo, B. Dong, Y. Qu, Z. Sun, L. Yang, Y. Wang, I. L. Fedushkin, X. J. Yang, *Chem. Eur. J.,* 2025, **31**, e202403652.
29 Y. Xie, C. Lu, B. Zhao, Q. Wang, Y. Yao, *J. Org. Chem.* 2019, **84**, 1951–1958.
30 Y. Shi, D. Wen, S. Q. Zhao, *Inorg. Chem.,* 2025, **64**, 4387–4392
31 W. Ding, X. Tang, S. Jin, Z. Li, D. Xu, X. Kang, Z. Liu, *Green Chem.,* 2024, **27**, 218–226
32 Y. Shi, B. Tang, X.-L. Jiang, Y.-E. Jiao, H. Xu, B. Zhao, *J Mater. Chem. A,* 2022, **10**, 4889–4894.
33 A. J. Plajer, C. K. Williams, *Angew. Chem. Int. Ed.*, 2022, **61**, e2021044952022.
34 K. Sieja, J. von Mach-Szczypiński, J. von Mach-Szczypiński, *Med. Pr.,* 2018, **69**, 317–323.
35 A. W. Demartino, D. F. Zigler, J. M. Fukuto, P. C. Ford, *Chem. Soc. Rev.,* 2017, **46**, 21–39.
36 R. Morales-Nava, M. Fernández-Zertuche, M. Ordóñez, *Molecules*, 2011, **16**, 8803–8814.
37 A. Khalaj, M. Khalaj, *J. Chem. Res.* 2016, **40**, 445–448.
38 A. Biswas, S. Hajra, *Adv. Synth. Catal.* 2022, **364,** 3035–3042.
39 M. Sengoden, G. A. Bhat, D. J. Darensbourg, *Green Chem.,* 2022, **24**, 2535–2541.

View Article Online
DOI: 10.1039/D5NJ03189C

40 L. Invernizzi, C. Damiano, E. Gallo, *Chem. Eur. J.*, 2025, **31**, e202500473.
41 S. Grimme, *J. Comp. Chem.,* 2006*,* **27***,* 1787-17991.
42 V. Barone, M. Cossi, *J. Phys. Chem. A*, 1998, **102**, 1995–20013.
43 M. Cossi, N. Rega, G. Scalmani, V. Barone, J. *Comp. Chem*., 2003, **24,** 669-681.
44 L. R. Domingo, M. Ríos-Gutiérrez, P. Pérez, *Molecules*, 2016, **21**, 7482016.
45 C. Damiano, N. Panza, J. Nagy, E. Gallo, G. Manca, *New J Chem.,* 2023*,* **47***,* 4306-4312.

UNIVERSITÀ DEGLI STUDI DI MILANO
DIPARTIMENTO DI CHIMICA

View Article Online
DOI: 10.1039/D5NJ03189C

Milano, 6th August 2025

Dear Editor,

The datasets supporting this article are included in the supporting information. Additional data are available from the corresponding author upon reasonable request.

Sincerely

Caterina Damiano

Dipartimento di Chimica, Direttore Prof. Luigi Lay
Via Golgi, 19 – 20133 Milano (Italy)
Tel: +39.0250314269 Fax: +39.0250314300 e-mail: direzione.dipchi@unimi.it